Thermochimica Acta, 207 (1992) 245–254
Elsevier Science Publishers B.V., Amsterdam

The examination of the phase transformation of aragonite into calcite by means of DSC analysis

J. Perić, R. Krstulović, T. Ferić and M. Vučak
Faculty of Technology, University of Split, Teslina 10 / V, 58000 Split, (Croatia)
(Received 9 December 1991)

Abstract

The X-ray diffraction method was used to determine the content of aragonite and calcite in samples of precipitated calcium carbonate synthesized in the laboratory. The transformation of the aragonite modification present into the stable calcite structure was traced by means of DSC analysis. All the samples were analysed by DSC under non-isothermal conditions in the temperature range 624–772 K at heating rates of 5, 10, 15, 20 and 25 K min^{-1}. A mathematical analysis of experimental DSC curves defined the mechanism and the kinetics of the phase transformation of aragonite into calcite. The kinetic curves $\alpha = f(t)$ and $\alpha = f(T)$ are sigmoidal in shape, and their inflection points and the v_m point of the curves $v = f(t)$ and $v = f(T)$ are interrelated and are defined by the concept of a stationary point.

The kinetic curves indicate that v_m corresponds to $(dH/dt)_m$ of the endothermal peak of transformation of aragonite into calcite, which is characteristic of a topochemical reaction.

INTRODUCTION

It is known that anhydrous calcium carbonate occurs in three crystal modifications: calcite, aragonite and vaterite. By varying the conditions of preparation, all three polymorphic modifications can be obtained selectively in comparatively pure states [1–6].

Aragonite and vaterite are metastable modifications which transform into the more stable calcite when heated [6–9]. Because each modification has a certain energy content, when one crystal modification transforms into another, a quantity of energy, equal to the difference between the energy contents of the two modifications, is released or captured.

In this research, the phase transformation of aragonite into calcite was followed by means of differential scanning calorimetry (DSC).

Correspondence to: J. Perić, Faculty of Technology, University of Split, Teslina 10/V, 58000 Split, Croatia.

EXPERIMENTAL

Two samples were prepared in the laboratory: sample A by precipitation of calcium carbonate from calcium nitrate and sodium carbonate solutions [1], and sample B by homogeneous precipitation of calcium carbonate from trichloroacetate medium [2].

Sample analysis

Chemical and mineralogical analysis

The calcium concentration was determined by complexometric titration at pH 12 with calcein indicator. The percentage of $CaCO_3$ was then calculated.

Qualitative and quantitative phase analysis of the samples was carried out in a Philips X-ray diffractometer with the following operating conditions: Cu Kα radiation was used, the scanning speed was 1 deg min^{-1}, the reduction factor RF was 400, and the time constant TC was 4.

DSC analysis

The DSC analysis was carried out under dynamic non-isothermal conditions and in a flow of extra-pure nitrogen in a Perkin–Elmer DSC-4 differential scanning calorimeter. The operating conditions were: temperature range, 623–773 K; heating rates, 5, 10, 15, 20 and 25 K min^{-1}; cooling rate, 593 K min^{-1}; and flow rate of extra-pure nitrogen, 30 ml min^{-1}.

The choice of the upper temperature limit of 773 K was influenced by the characteristics of the apparatus.

RESULTS AND DISCUSSION

Mineralogical analysis of samples

Based on X-ray patterns (Fig. 1) and the $CaCO_3$ content of the samples, the quantitative analysis (the matrix-flushing method according to Chung [10]) determined the amount of aragonite and calcite for the most intense diffraction lines of aragonite ($d_{111} = 0.340$) and calcite ($d_{104} = 0.303$). Table 1 presents the results of the analysis.

Differential scanning calorimetry

The phase transformation of aragonite into calcite is an endothermal process

$$A \xrightarrow{\text{heat}} C + \Delta H$$

which can be seen in the DSC curves (Figs. 2 and 3) by the presence of an

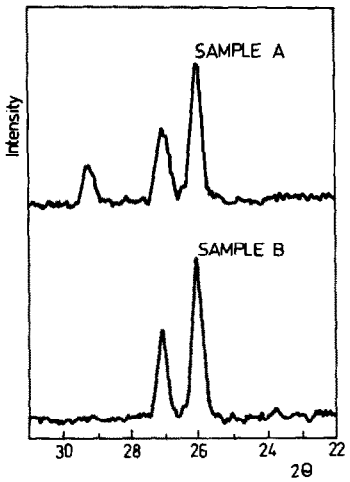

Fig. 1. X-ray patterns for samples A and B.

TABLE 1

Results of the chemical and mineralogical analysis of the samples

Sample	$CaCO_3$ (%)	Aragonite (%)	Calcite (%)
A	95.61	95	5
B	97.20	100	0

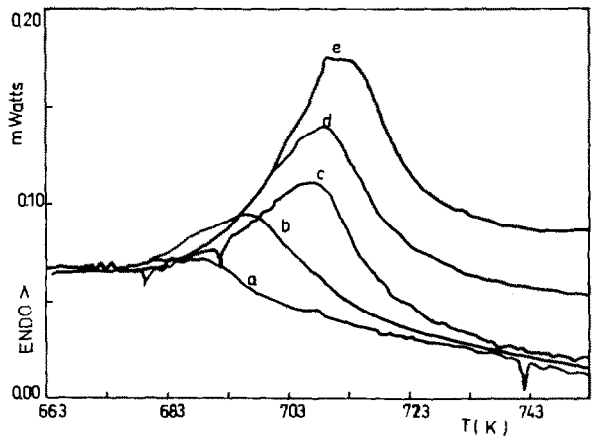

Fig. 2. DSC curves for sample A. Heating rates: curve a, 5 K min^{-1}; curve b, 10 K min^{-1}; curve c, 15 K min^{-1}; curve d, 20 K min^{-1}; curve e, 25 K min^{-1}.

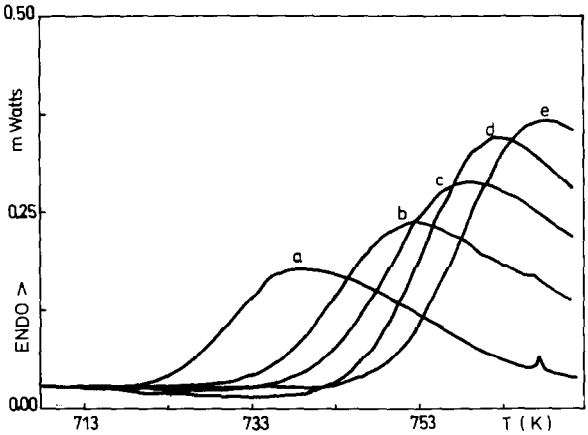

Fig. 3. DSC curves for sample B. Curves as for Fig. 2.

endothermal peak in the temperature range 683–772 K.

When the heating rate is increased from 5 to 25 K min^{-1}, the endothermal peak increases, and its maximum shifts towards higher temperatures. With sample B, these effects do not end in the operating temperature range.

Mathematical elaboration of the DSC curves

The DSC curves were elaborated mathematically in order to determine the mechanism and the kinetics of the phase transformation of aragonite into calcite by means of methods using a number of experimental kinetic curves and the stationary point theory [11]. The degree of transformation α is determined from the ratio of change of enthalpy $\Delta H_{\text{partial}}$ in time t and the change of total enthalpy ΔH_{total}

$$\alpha = \frac{\Delta H_{\text{partial}}}{\Delta H_{\text{total}}} \tag{1}$$

i.e. by determining the partial and total surface of the DSC curve.

The phase transformation rate v is expressed as a differential change

$$v = \left(\frac{\mathrm{d}\alpha}{\mathrm{d}t}\right) \tag{2}$$

and represents a function of α and time t [12]. Figures 4 and 5 show graphically the dependence of the calculated values of α on temperature and time for sample A. It can be seen that the curves $\alpha = f(t)$ and $\alpha = f(T)$ are sigmoidal in shape for different heating rates (Figs. 4 and 5). With non-isothermal curves $\alpha = f(t)$, the degree of transformation α is zero at zero time (the beginning of change), which would indicate that this process is not characterized by an induction period.

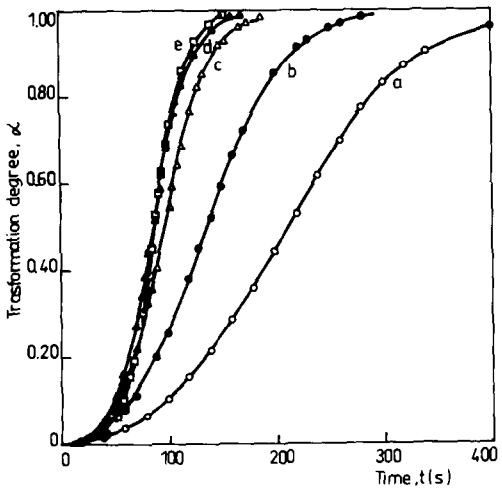

Fig. 4. Plots of degree of transformation versus time for sample A. Curves as for Fig. 2.

Figures 6 and 7 show graphically the dependence of transformation rate on time and temperature for sample A. It can be seen that when the heating rate decreases, the maximum rate v_m shifts towards longer times, i.e. the maximum rate is obtained in shorter periods when heating rates are higher.

Curves of the dependences $\alpha = f(t, T)$ and $v = f(t, T)$ for sample B show similar shapes to those for sample A. Application of these dependences in further mathematical analyses, i.e. the calculation of kinetic

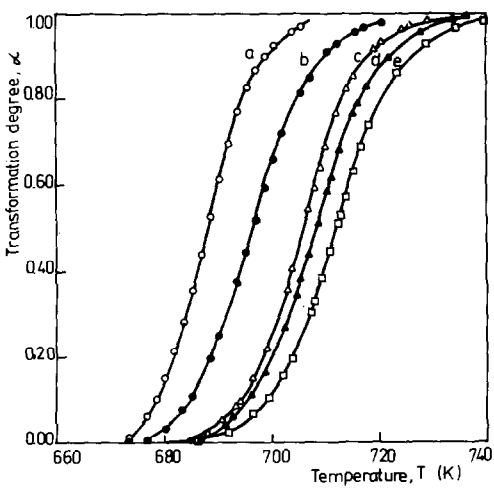

Fig. 5. Plots of degree of transformation versus temperature for sample A. Curves as for Fig. 2.

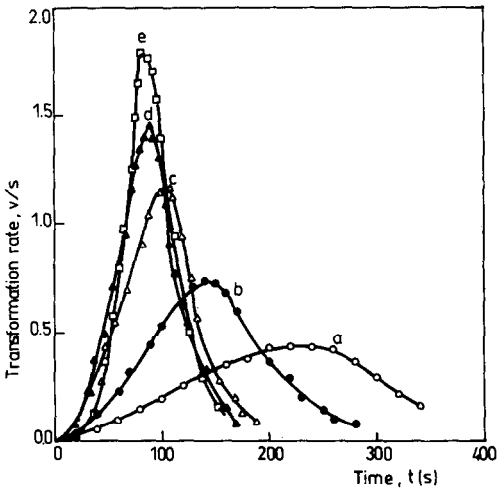

Fig. 6. Plots of transformation rate versus time for sample A. Curves as for Fig. 2.

parameters, was restricted to methods using the heating rate q, temperature T_m and time t_m at which the maximum transformation rate v_m is achieved, that is, those parameters which can be determined exactly enough, even though the endothermal effects do not end in the operating temperature range. The degree of transformation α, and therefore its differential change, were not calculated precisely, because the change in total enthalpy ΔH_{total} could not be determined.

The activation energy was calculated for samples A and B by means of several methods of non-isothermal kinetics derived from the stationary

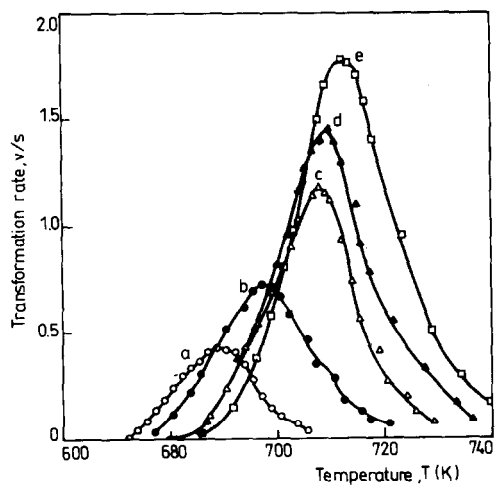

Fig. 7. Plots of transformation rate versus temperature for sample A. Curves as for Fig. 2.

point theory [11]
the Antić–Colović method

$$\frac{\mathrm{d}\ln v_m}{\mathrm{d}(1/T_m)} = -\frac{E}{R} \tag{3}$$

the Kissinger method

$$\frac{\mathrm{d}\ln(q/T_m^2)}{\mathrm{d}(1/T_m)} = -\frac{E}{R} \tag{4}$$

the modified Kissinger method

$$\frac{\mathrm{d}\ln(q/T_m)}{\mathrm{d}(1/T_m)} = -\frac{E}{R} \tag{5}$$

the Ozawa method

$$\frac{\mathrm{d}\ln q}{\mathrm{d}(1/T_m)} = -\frac{E}{R} \tag{6}$$

where E is the activation energy (J mol^{-1}), R the gas constant (J mol^{-1} K^{-1}), q the linear heating rate (K s^{-1}), v_m the maximum transformation rate, and T_m and t_m the temperature and time at which v_m is achieved.

The slopes of the straight lines drawn by a least-squares method (obtained by plotting $\ln v_m$, $\ln(q/T_m^2)$, $\ln(q/T_m)$ and $\ln q$ versus $1/T_m$) determine the values of activation energy.

Because the kinetic curves $\alpha = f(t)$ and $\alpha = f(T)$ are sigmoidal in shape, and because the curves $\alpha = f(t_{red})$ overlap for different heating rates (Fig. 8), the modified Kazeev–Erofeev equation [11] (eqn. (7)), can be used to determine the pre-exponential factor k_0 of the Arrhenius equation and the kinetic parameter n by the least-squares method

$$\frac{E}{RT_m} = \ln k_0 - \ln[-\ln(1-\alpha_m)] + n \ln t_m \tag{7}$$

where α_m is the degree of transformation in the stationary point, i.e. at the moment of achieving the maximum reaction rate.

Table 2 compares the calculated values for activation energy and kinetic parameters of the phase transformation of aragonite into calcite for samples A and B. Table 2 shows that activation energy values calculated by means of eqns. (4)–(6) show good correspondence, while the activation energy calculated by means of eqn. (3) is significantly lower; therefore this value was not taken into account when determining the average activation energy. It can also be seen that sample B, consisting of pure aragonite, has a somewhat higher activation energy than sample A which contains 95% aragonite and 5% calcite. This may be due to the different methods of

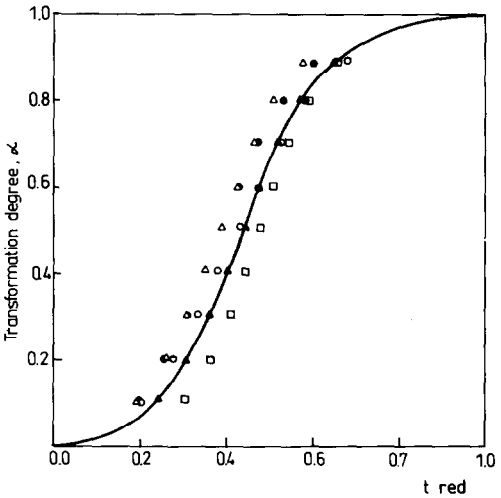

Fig. 8. Affine transformed curves for the phase transformation of aragonite into calcite. Heating rates: ○, 5 K min^{-1}; ●, 10 K min^{-1}; △, 15 K min^{-1}; ▲, 20 K min^{-1}; □, 25 K min^{-1}. $t_{red} = t_i / t_f$, where t_i is the current time and t_f the final time of the reaction development under non-isothermal conditions for the corresponding heating rate.

sample preparation, as well as to the presence of calcite in sample A which favours the phase transformation of aragonite into calcite [2].

CONCLUSIONS

A characteristic endothermal peak of the phase transformation A → C occurs in the temperature range 683–772 K. If the heating rate is increased from 5 K min^{-1}, the endothermal peak increases, and its maximum shifts towards higher temperatures, so that these effects do not end in the operating temperature range for sample B.

An analysis of the kinetic curves $\alpha = f(t)$ and $\alpha = f(T)$ shows that they are sigmoidal in shape. With curves $\alpha = f(t)$, if the heating rate increases, the time needed to achieve the same degree of transformation α becomes shorter; with curves $\alpha = f(T)$, the same degree of transformation is obtained at lower temperatures, if the heating rate is lower.

The kinetic curves show that v_m corresponds to $(dH/dt)_m$ of the endothermal peak, which characterizes topochemical reactions. The maximum transformation rate is obtained in a shorter period at higher heating rates.

With curves $v = f(T)$, it can be seen that when the heating rate increases, the maximum transformation rate increases and shifts towards higher temperatures.

The activation energy values for the phase transformation, calculated for samples A and B by means of several methods of non-isothermal kinetics

TABLE 2

Values of kinetic parameters in the phase transformation of aragonite into calcite

Method applied	Sample							
	A				B			
	E_a (kJ mol^{-1})	E_a (ave) (kJ mol^{-1})	n	$k_0 \times 10^{-17}$ (s^{-1})	E_a (kJ mol^{-1})	E_a (ave) (kJ mol^{-1})	n	$k_0 \times 10^{-17}$ (s^{-1})
Antić–Colović	251.6				–			
Kissinger	264.2				283.9			
Modified Kissinger	270.1	270.1	1.148	1.10	290.2	290.2	0.858	3.59
Ozawa	275.9				296.4			

derived from the stationary point theory, show good correspondence. The activation energy values for sample A, consisting of 95% aragonite and 5% calcite, are somewhat lower, which may be explained by the presence of the calcite modification which favours the phase transformation of aragonite into calcite.

REFERENCES

1 J.L. Wray and F. Daniels, J. Am. Chem. Soc., 79 (1957) 2031.
2 M. Subba Rao and S.R. Yoganarasimhan, Am. Mineral., 50 (1965) 1489.
3 H. Yamada and N. Hara, Gypsum and Lime, 203 (1986) 221.
4 H. Yamada and N. Hara, 1st Int. Conf. on Ceramic Powder Processing Science, INC. Orlando, FL, 1987, Ceramic Transactions, Vol. 1, pp. 39–46.
5 H.R. Langelin, A. Delannoy, J. Nicole and J. Hennion, Inf. Chim., 252/253 (1983) 135.
6 D. Kralj, Lj. Brečević and A.E. Nielsen, J. Cryst. Growth, 104 (1990) 793.
7 B.L. Davis and L.H. Adams, J. Geophys. Res., 70 (1965) 433.
8 W.S. Fyfe and J.L. Bischoff, in L.C. Pray and R.C. Murray (Eds.), Society of Economic Paleontologists and Mineralogists, Special Publication No. 13, 1964, pp. 3–13.
9 M. Subba Rao, Indian J. Chem., 11 (1973) 280.
10 S. Popović, B. Gržeta and T. Balić-Žunić, Kem. Ind., 36 (1987) 1.
11 M. Antić and N. Colović, Kinetika heterogenih hemijskih reakcija, Institut zaštite na radu, Niš, 1983, pp. 269–278, 285–390.
12 DSC-4 Standard Program manual (Perkin–Elmer Part No. 0993-9823).